Riboflavin-Functionalized Cerium Fluoride Nanoparticles Induced Mitochondrial Dysfunction in Melanoma Cells Under UV Irradiation

Nikita Chukavin , Uliana Andreeva , Anton Popov *

Posted Date: 20 January 2025

doi: 10.20944/preprints202501.1399.v1

Keywords: cerium fluoride nanoparticles; riboflavin; photosensitizers; photodynamic therapy

Article

Riboflavin- Functionalized Cerium Fluoride Nanoparticles Induced Mitochondrial Dysfunction in Melanoma Cells Under UV Irradiation

Chukavin N.N. [1], Andreeva U.O. [2] and Popov A.L. [1,*]

[1] Institute of Theoretical and Experimental Biophysics of the Russian Academy of Sciences, Pushchino, Russia

[2] Manipal Academy of Higher Education, Dubai, UAE

* Correspondence: antonpopovleonid@gmail.com

Abstract: One of the current approaches to improve the effectiveness of photodynamic therapy (PDT) is the development of advanced photosensitizers, including those based on nanoparticles. In this research, we have demonstrated for the first time the possibility of using the cerium fluoride nanoparticles, functionalized with riboflavin (Rb-CeF_3 NPs), as a nanophotosensitizer for PDT. The binding of riboflavin to CeF_3 NPs results in the stabilization of these nanoparticles and does not lead to the formation of an amorphous structure. At the same time, the Rb-CeF_3 NPs exhibit a pronounced absorption of light at a wavelength of 450 nm, similar to pure riboflavin. The Rb-CeF_3 NPs show remarkable cytotoxicity to B16/F10 mouse melanoma cells through a mitochondria-dependent mechanism. The light irradiation at a wavelength of 450 nm notably reduces both the cell viability of B16/F10 cells and their mitochondrial membrane potential. The Rb-CeF_3 NPs significantly improve this effect, thereby demonstrating a pronounced photosensitizing activity of these nanoparticles. However, there is no significant difference in the effect of riboflavin and Rb-CeF_3 NPs under light irradiation. Therefore, we propose, that CeF_3 NPs are mainly a cargo for riboflavin, which can stabilize and deliver it to tumor cells for the purposes of PDT. Various modifications of the Rb-CeF_3 NPs synthesis technique, changes in the ratio of components, selection of different light irradiation conditions may enhance the photosensitizing properties of this nanomaterial.

Keywords: cerium fluoride nanoparticles; riboflavin; photosensitizers; photodynamic therapy

1. Introduction

Photodynamic therapy (PDT) is a relatively novel disease treatment approach utilized for the management of a wide variety of pre-malignant (such as actinic keratosis), malignant (such as lung, cervical, gastric and oesophageal cancer) and non-malignant (such as psoriasis) conditions [1–4]. Despite the fact that PDT has advantages over other therapeutic modalities for cancer, including chemotherapy, radiotherapy and surgery, such as non-invasiveness, high accuracy, negligible adverse effects, lowered toxicity regarding healthy tissues as well as excellent cosmetic effects, this kind of cancer treatment remains not broadly used in the clinic [1,3–5]. There are several factors that actually hinder the development and effective use of PDT, including limitations of light penetration through the tissues, lowered oxygenation of tumors as well as unsatisfying properties of photosensitizers, chemicals, which interact with light thus providing the effect of PDT [1,2]. In particular, photosensitizers may exhibit low solubility and bioavailability, decreased target specificity together with inappropriate quantum yield and non-tissue penetrating activating light wavelength [1,2,4]. To overcome these limitations, novel approaches are being developed to bind photosensitizers with various nanoparticles [6–8].

Use of ceria-based nanoparticles (nanoceria) is a promising approach for overcoming the limitations of photosensitizers applied in clinics. This is due to the unique physico-chemical properties of ceria nanoparticles, which endow them with remarkable biological activity and the

 doi:10.20944/preprints202501.1399.v1

possibility of surface functionalization for targeted accumulation in tumor cells [9,10]. Moreover, ceria-based nanoparticles are able to enhance the therapeutic effects of photosensitizers through improving their uptake and retention in tumors together with increasing the production of reactive oxygen species (ROS) [11,12]. Additionally, nanoceria can be functionalized with fluorescent probes, such as calcein, to endow them with a diagnostic feature of ROS detection [13,14]. Cerium fluoride nanoparticles (CeF_3 NPs) is one of the representatives of the ceria nanoparticles. CeF_3 nanoparticles exhibit a pronounced optical absorption in the UV-region of the light spectrum, which makes them a promising candidate for use in combination with photosensitizers in PDT [15]. In particular, CeF_3 NPs can transfer the energy from UV-irradiation directly to a photosensitizer, thereby enhancing its therapeutic effect [16]. Meanwhile, CeF_3 nanoparticles can be doped with terbium ions (Tb^{3+}), which in turn causes the effective energy transfer from cerium to terbium ions within the crystal lattice, thus enhancing the luminescent properties of the doped nanoparticles [15,17,18]. Furthermore, it has been demonstrated, that such luminescent features can also be used for the excellent visualization of cells and enamel defect zones [15,19]. In addition, doping of CeF_3 NPs with Yb and Tm ions endow them with a property of identification and detection of vulnerable atherosclerosis plaques [20]. It is worth noting, that CeF_3 NPs are able to exhibit selective effect on tumor and healthy cells under X-ray irradiation [21] Thus, cerium fluoride nanoparticles hold great promise for binding and delivering photosensitizers in order to enhance the effectiveness of PDT.

Riboflavin (Rb), also known as vitamin B2, is of particular interest for PDT, due to its remarkable photosensitizing activity [22] By absorbing the energy from UV-irradiation, riboflavin is able to perform photosensitization of I and II types, generating a wide variety of ROS in cells [23]. The photosensitizing effect of riboflavin has been used in a wide range of biomedical applications, including PDT [24–28]. Meanwhile, riboflavin is able to selectively accumulate in different tumor cells, including breast cancer, squamous cell carcinoma, glioma and melanoma cells, due to overexpression of riboflavin receptors and transporters on their surface [29,30]. Despite all the advantages, riboflavin has a number of features, limiting its use in PDT, including low solubility in water, restricted stability and tissue penetration, necessity of activation by visible light as well as decreased quantum yield [31–35]. Currently, riboflavin is being increasingly conjugated with various molecules and nanocarriers, which makes it possible to overcome the disadvantages mentioned above [29,35,36]. In particular, it has been shown, that the binding of riboflavin with silver nanoparticles (Ag NPs), coated with pectin, leads to an enhancement of its photosensitizing effect on HeLa cells [23]. In another study, it has also been demonstrated, that the conjugation of riboflavin with silver Ag NPs caused an increase in the level of ROS, produced under light irradiation [37]. Therefore, riboflavin can be used as an effective photosensitizer, and its limitations can be mitigated by its binding with nanoparticles.

In this study, we have for the first time demonstrated the potential of using cerium fluoride nanoparticles functionalized with riboflavin (Rb-CeF_3 NPs) as a nanophotosensitizer for photodynamic therapy.

2. Materials and methods

2.1. Synthesis of Riboflavin-Functionalized CeF_3 Nanoparticles

Rb-CeF_3 NPs were synthesized as follows: 5 mmol of cerium chloride heptahydrate was loaded into a 250 ml plastic cup and dissolved in 15 ml of deionized water, after that 150 ml of isopropyl alcohol was added to the solution. Separately, 40 mmol HF (0.742 ml in terms of 38% hydrofluoric acid) was dissolved in 50 ml of isopropyl alcohol in a plastic cup. The first cup was placed on a magnetic stirrer, and then the HF solution was added, drop by drop, from the second cup, while continuously stirring. After adding the entire volume of HF solution, the stirring was continued for 15 min. Then 0.0133 mmol of riboflavin was added to form Rb-CeF_3 NPs, and the stirring was continued for an additional 15 min. Following this, the stirring was stopped, and the resulting yellow precipitate was filtered using a funnel and a paper filter. The filtrate was washed several times with

 doi:10.20944/preprints202501.1399.v1

small amounts of isopropyl alcohol to remove any traces of HCl and HF. After that, the filter was transferred to a Petri dish and placed in an ED 115 heating chamber (BINDER, Germany) at 70 °C for 4 hours. The dried sample was transferred to a glass and redispersed in 110 ml of deionized water, thereby forming yellow stable sol. Following this, water sol of Rb-CeF_3 NPs was washed routinely by dialysis.

2.2. Physico-Chemical Analysis

Size, shape and chemical composition of the Rb-CeF_3 NPs were analyzed using a NVision 40 scanning electron microscope (Carl Zeiss, Germany) equipped with an X-MAX detector (80 mm^2) (Oxford Instruments, United Kingdom) at an accelerating voltage of 20 kV. X-ray diffraction (XRD) of the nanoparticles was measured using a D8 Venture X-ray diffractometer (Bruker, Germany). Optical absorption of Rb-CeF_3 NPs in aqueous sol was measured using a Cary 5000 UV-vis spectrophotometer (Agilent Technologies, USA). Distribution of hydrodynamic diameter of the Rb-CeF_3 NPs in deionized water was determined using a N5 submicron particle size analyzer (Beckman Coulter, USA) at 25 °C.

2.3. Cell Culture

For cell culture experiments, B16/F10 mouse melanoma cells were obtained from the cryostorage of the Theranostics and Nuclear medicine lab (ITEB RAS, Russia). The B16/F10 cell line was selected due to its remarkable sensitivity to riboflavin, caused by the overexpression of riboflavin-specific transporters and receptors in these cells [38–40]. Cells were cultured in DMEM medium (PanEco, Russia), containing 4.5 g/L of D-glucose, 2 mM of L-glutamine, 100 U/mL of penicillin, 100 μg/mL of streptomycin (PanEco, Russia) and 10% of Fetal Bovine Serum (FBS) (HyClone, USA). Cell culture experiments were performed using Neoteric laminar boxes (Lamsystems, Russia). Cells were incubated in CO_2-incubator D180 (RWD Life Science, China) at 37 °C in humidified atmosphere containing 5% CO_2. As cells grew and reached subconfluent state, they were treated with a 0.25% trypsin-EDTA (PanEco, Russia) solution and passed into new T12, T25 or T75 cell culture flasks (SPL Life Sciences, Korea) at a ratio of 1:4. Before conducting experiments with the nanoparticles, cells were seeded on 96-well plates (SPL Life Sciences, Korea) at a density of 25000 cells/cm^2 and cultivated for 24 hours. Following this, cell culture medium was replaced with fresh medium, containing Rb-CeF_3 NPs at different concentrations for subsequent co-incubation, lasting 24, 48 and 72 hours.

2.4. Laser Light Irradiation

A device was designed to irradiate cells with a 450 nm laser in order to study the effect of laser light irradiation on B16/F10 cells and to determine the possible photosensitizing activity of Rb-CeF_3 NPs under respective conditions (Figure S1). Briefly, an optimal distance (l) from the fiber tip of the 450 nm laser Alta-Blue (IRE-Polus Ltd., Russia) to the bottom of the plate wells was determined by considering several parameters, including a diameter of the irradiated spot (D) equal to 13 cm, which contains the working area on the plate (6.5 cm), and a numerical aperture of the laser fiber (NA) equal to 0.22, which was calculated as the tangent of the maximum incident angle of the laser beam with respect to the fiber axis. According to the formula NA=D/2*l (a diameter of the aperture d can be neglected), the optimal distance l is 29.54 cm. The following experimental laser powers were selected for the irradiation of cells: 1, 3, 6, 9 and 13 W, while only 3, 9 and 13 W were used in the experiments with nanoparticles. After 48 hours of cultivation without nanoparticles or 24 hours after co-incubation with Rb-CeF_3 NPs at a concentration of 0.5 mM, cells were irradiated using the designed device for 10 min.

 doi:10.20944/preprints202501.1399.v1

2.5. Cell Viability Assay

Cell viability assay was performed by routine MTT-assay 24, 48 and 72 hours after co-incubation with Rb-CeF_3 NPs or 24 hours after laser light irradiation. Briefly, cell culture medium was replaced with a solution of MTT (3-(4,5-dimethylthiazole-2-yl)-2,5-diphenyl-tetrazolium bromide) (PanEco, Russia) in a serum-free medium at a concentration of 0.5 mg/mL. This assay is based on the principle, that yellow soluble MTT is being reduced by intracellular NAD(P)H-dependent oxidoreductase enzymes to purple insoluble formazan-derivative depending on the metabolic activity of cell and, consequently, its viability. After 3 hours of incubation, the residual MTT solution was replaced with DMSO (PanEco, Russia) in order to dissolve intracellular formazan, and then plate was placed on a plate shaker for 1 minute. After that, an optical density (OD) of the resulted solutions was measured at a wavelength of 570 nm using an INNO-S plate reader (LTek, Korea). The OD values were recalculated as a percentage of the corresponding values from the control groups, the results were presented as a Mean ± Standard deviation (SD).

2.6. Analysis of Mitochondrial Membrane Potential

Mitochondrial membrane potential (MMP) analysis was performed 24, 48 and 72 hours after co-incubation with Rb-CeF_3 NPs or 24 hours after laser light irradiation. Briefly, cell culture medium was replaced with a TMRE solution (tetramethylrodamine, ethyl ether) (Lumiprobe, Russia), which selectively accumulates in active mitochondria due to their transmembrane potential (Ex=550 nm, Em=575 nm), in a HBSS at a concentration of 1 uM. After 15 minutes of incubation, cells were washed twice with HBSS, and then microphotography of the cells was carried out using ZOE fluorescent cell imager (Bio-Rad, USA). The fluorescence intensity of TMRE was measured using an ImageJ software and then recalculated as a percentage of the corresponding values from the control groups. Results were presented as a Mean ± Standard deviation (SD).

2.7. Cell Death Analysis

Cell death analysis was performed by routine Live/Dead assay 24, 48 and 72 hours after co-incubation with Rb-CeF_3 NPs. Briefly, cell culture medium was replaced with a mixture of fluorescent dyes Hoechst 33342 (Lumiprobe, Russia), which binds to the DNA of all of the cells (Ex=350 nm, Em=460 nm), and propidium iodide (PI) (Lumiprobe, Russia), which binds to the DNA of only dead cells (Ex=535 nm, Em=615 nm), dissolved in a Hanks' Balanced Salt Solution (HBSS) (PanEco, Russia) at a concentration of 1 uM. After 15 minutes of incubation, cells were washed twice with HBSS, and then microphotography of the cells was carried out using ZOE fluorescent cell imager (Bio-Rad, USA). Total number of the cells and number of the dead cells were counted using an ImageJ software. After that, percentage of the dead cells was calculated.

2.8. Statistical Analysis

Statistical analysis was performed using GraphPad Prism software. Significance of deviations between the experimental and control groups was confirmed using Welch's t-test with the corresponding p values: $0.01 < p < 0.05$ (*), $0.001 < p < 0.01$ (**), $0.0001 < p < 0.001$ (***) and $p < 0.0001$ (****).

3. Results and Discussion

According to the scanning electron microscopy data, the synthesized Rb-CeF_3 NPs have a size distribution ranging from 10 to 50 nm and have a spherical shape (Figure 1a). The XRD analysis confirms the crystal structure of Rb-CeF_3 NPs (Figure 1b), which is consistent with a CeF_3 NPs hexagonal structure with P63/mcm space group, that has been shown previously [21]. Therefore, the binding of CeF_3 NPs to riboflavin do not lead to the formation of an amorphous structure with unpredictable properties. The EDX results demonstrate the actual chemical composition of the

 doi:10.20944/preprints202501.1399.v1

obtained Rb-CeF_3 NPs (Figure 1c), which corresponds to the proposed structure (Al and Cu were present in a sample holder). The optical absorption spectra of the CeF_3 NPs and Rb-CeF_3 NPs reveal, that the binding of riboflavin to CeF_3 NPs causes an increase in its optical absorption at 450 nm (Figure 1d). This phenomenon proves the possibility of photoactivating these nanoparticles using light with a wavelength of 450 nm. The distributions of the hydrodynamic size of CeF_3 NPs (Figure 1e) and Rb-CeF_3 NPs (Figure 1f) exhibit two main peaks at 104 and 234 nm and at 84 and 198 nm, respectively. Meanwhile, there are many particles with an intermediate size ranging from 84 to 198 nm in the presence of riboflavin. Hence, the binding of riboflavin causes the simultaneous reduction in the CeF_3 NPs size and the increase in their polydispersity, which is consistent with SEM data. We assume that this phenomenon could be due to the stabilization of CeF_3 NPs by riboflavin.

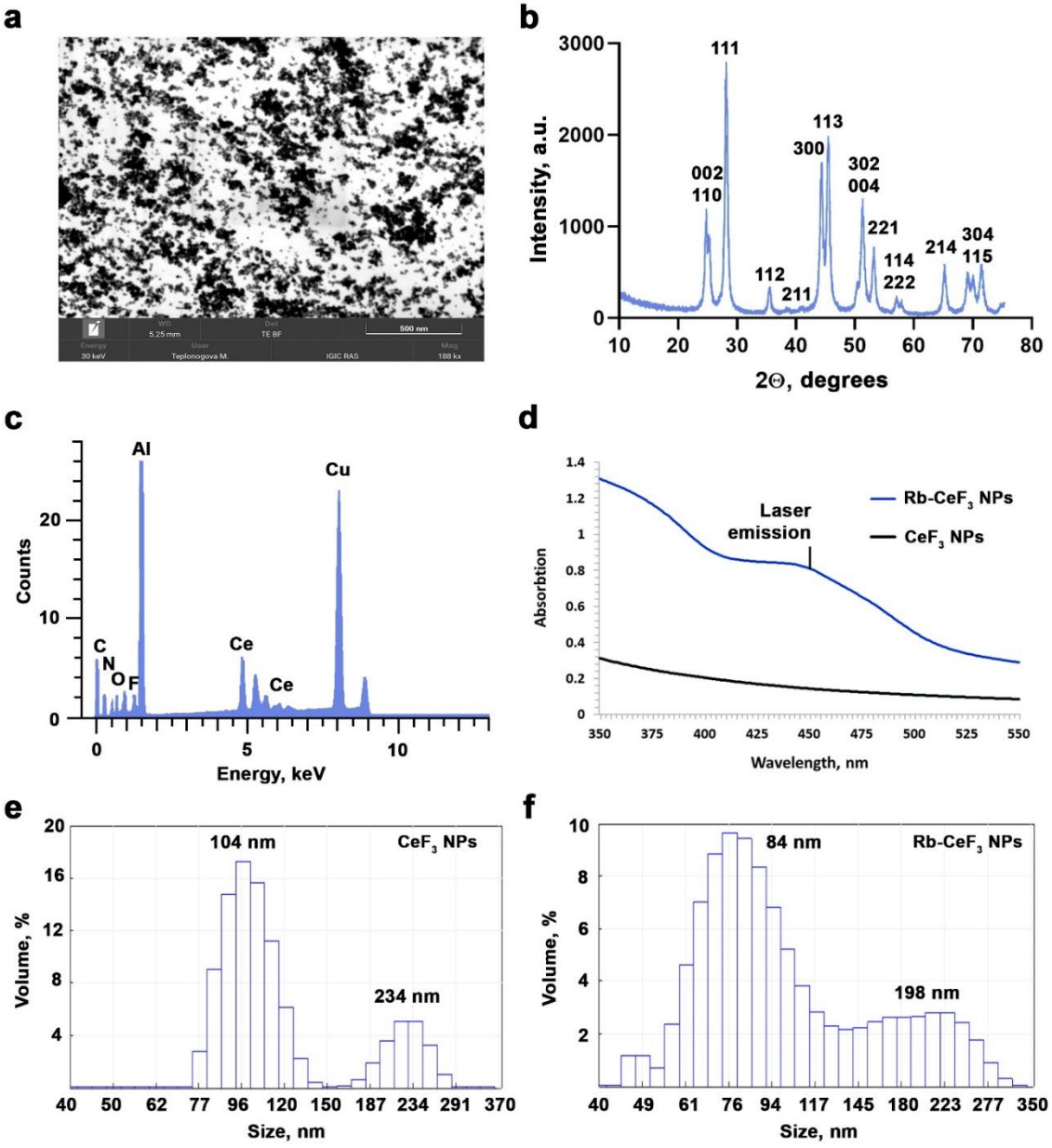

Figure 1. Physico-chemical properties of the Rb-CeF_3 NPs. SEM image (a), XRD pattern (b), EDX (c) and optical absorption spectra (d) of the Rb-CeF_3 NPs. Distributions of the hydrodynamic size of CeF_3 NPs (e) and Rb-CeF_3 NPs (f) in deionized water, obtained by DLS.

According to the cell viability assay data (Figure 2a), both CeF_3 NPs and Rb-CeF_3 NPs exhibit a remarkable cytotoxicity to B16/F10 mouse melanoma cells. It is worth noting, that the effect of CeF_3

 doi:10.20944/preprints202501.1399.v1

NPs on the viability of these cells is more pronounced than that of Rb-CeF_3 NPs after 24 and 48 hours of co-incubation. However, the cytotoxicity of Rb-CeF_3 NPs slightly exceeds that of the unfunctionalized nanoparticles after 72 hours of co-incubation. Meanwhile, the effect of the studied nanoparticles on the MMP of B16/F10 cells differs significantly: CeF_3 NPs do not dramatically change the MMP, while Rb-CeF_3 NPs decrease it in a dose-dependent manner, and this effect enhances during 72 hours of co-incubation (Figures 2b and 2c). At the same time, neither CeF_3 NPs nor Rb-CeF_3 NPs induce cell death at all studied concentrations during the entire co-incubation period (Figure S2). Consequently, the functionalization of CeF_3 NPs with riboflavin alters the mechanism of cytotoxicity towards B16/F10 mouse melanoma cells to a mitochondria-dependent one. Nevertheless, it does not ensure the development of cell death in the presence of these nanoparticles.

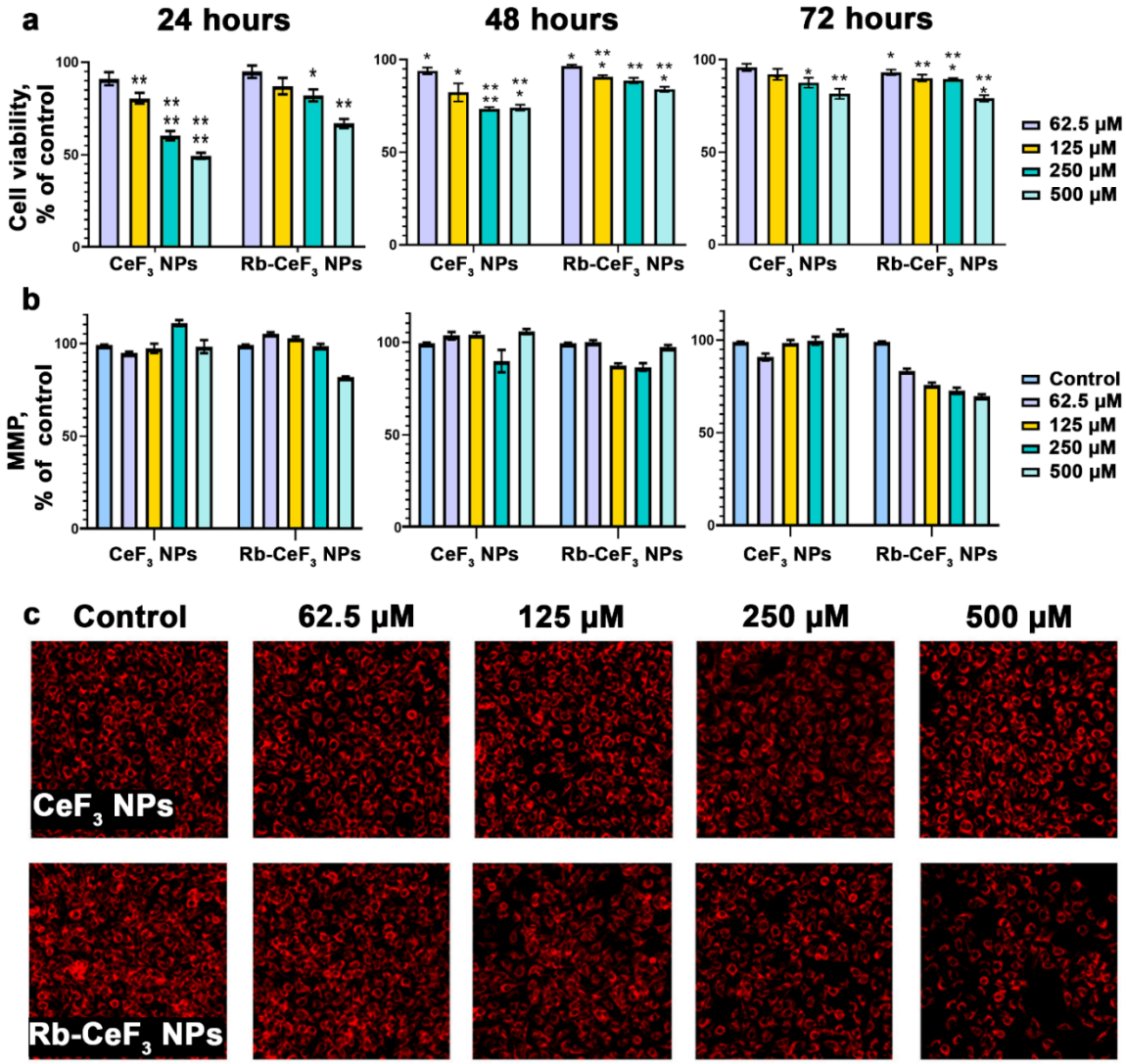

Figure 2. Cytotoxicity of the Rb-CeF_3 NPs to B16/F10 mouse melanoma cells. Effect of Rb-CeF_3 NPs and CeF_3 NPs at different concentrations on the cell viability (a) and mitochondrial membrane potential (MMP) (b, c) of B16/F10 cells after 24, 48 and 72 hours of co-incubation. Results in the diagrams (a,b) are presented as a percentage of control with Mean ± SD, n=3. Statistical significance of the differences between the control and experimental groups was confirmed using Welch's t-test with corresponding p values: $p < 0.05$ (*), $p < 0.01$ (**), $p < 0.001$ (***) and $p < 0.0001$ (****). Cells, shown in the images (c), are stained with TMRE, MMP-dependent dye.

Interestingly, that the light irradiation with a wavelength of 450 nm significantly decreases both the cell viability and the MMP of B16/F10 mouse melanoma cells in a power-dependent manner (Figures 3a, 3c and 3e). This effect may be due to the intense accumulation of various chromophores,

 doi:10.20944/preprints202501.1399.v1

including flavins and porphyrins, in melanoma cells [41]. Further, to assess the photosensitizing effect of Rb-CeF_3 NPs and their components, a concentration of 500 μM has been chosen. Surprisingly, that CeF_3 NPs alone do not influence the effect of light irradiation on B16/F10 cells, despite the investigated cytotoxicity of these nanoparticles. However, both riboflavin and Rb-CeF_3 NPs demonstrate a remarkable photosensitizing activity, decreasing the cell viability and the MMP of the cells, regardless of the laser power (Figures 3b, 3d, 3f and S3). It is obvious, that the binding of riboflavin to CeF_3 NPs do not affect its photosensitizing activity neither decreasing nor increasing it. Hence, we propose, that CeF_3 NPs are mainly cargo for riboflavin, which can stabilize and deliver it to tumor cells for the purposes of PDT. Various modifications of the Rb-CeF_3 NPs synthesis technique, changes in the ratio of components, selection of different light irradiation conditions may enhance the photosensitizing properties of this nanomaterial.

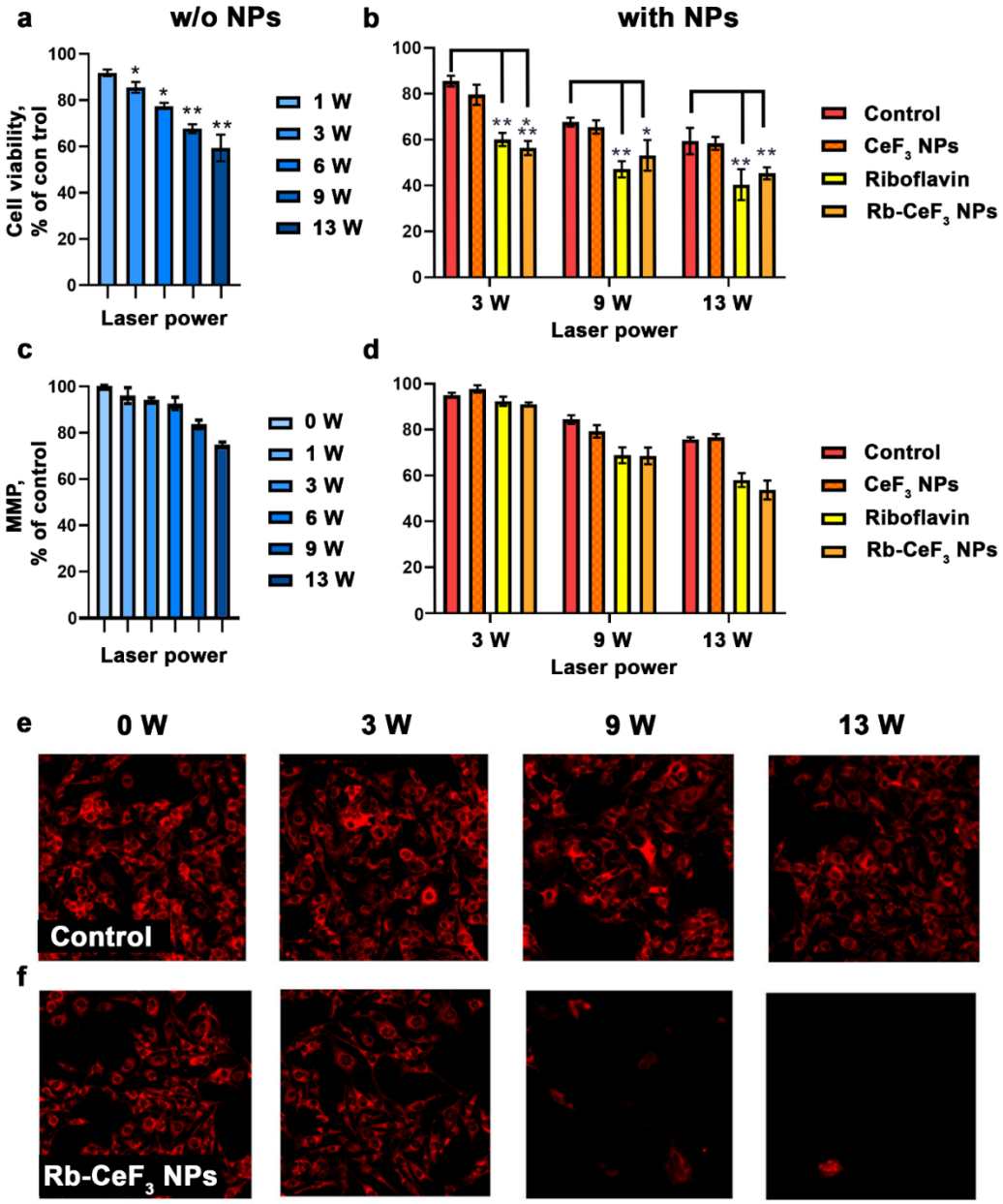

Figure 3. Effect of 450 nm-laser light irradiation on B16/F10 cells and photosensitizing activity of the Rb-CeF_3 NPs under respective conditions. Changes in cell viability (a) and mitochondrial membrane potential (MMP) (b, c) of B16/F10 cells under laser light irradiation with different laser power in the absence (left) and presence (right) of Rb-CeF_3 NPs and its components at a concentration of 500 μM 24 hours after irradiation. 24 hours before light irradiation, cells were cultivated in the absence or presence of the Rb-CeF_3 NPs for 24 hours. Results in the

 doi:10.20944/preprints202501.1399.v1

diagrams (a, b) are presented as a percentage of control with Mean ± SD, n=3. Statistical significance of the differences between control and experimental groups was confirmed using Welch's t-test with corresponding p values: $p < 0.05$ (*), $p < 0.01$ (**), $p < 0.001$ (***) and $p < 0.0001$ (****). Cells, shown in the images (c), are stained with TMRE, MMP-dependent dye.

4. Conclusion

One of the modern approaches to enhance the effectiveness of photodynamic therapy (PDT) is the development of advanced photosensitizers, including those based on nanoparticles. In this study, we have for the first time showed the potential of using the cerium fluoride nanoparticles, functionalized with riboflavin (Rb-CeF_3 NPs), as a nanophotosensitizer for PDT. The binding of riboflavin to CeF_3 NPs leads to the stabilization of these nanoparticles and does not cause the formation of an amorphous structure with unpredictable features. Meanwhile, the Rb-CeF_3 NPs are able to intensively absorb the light with a wavelength of 450 nm, similar to pure riboflavin. The Rb-CeF_3 NPs exhibit pronounced cytotoxicity towards B16/F10 mouse melanoma cells through a mitochondria-dependent mechanism. The light irradiation at a wavelength of 450 nm significantly decreases both the cell viability and the mitochondrial membrane potential of B16/F10 cells. The Rb-CeF_3 NPs notably enhance this effect, therefore demonstrating a remarkable photosensitizing activity of these nanoparticles. However, there is no important difference in the effect of riboflavin and Rb-CeF_3 NPs under light irradiation. Thus, we assume, that CeF_3 NPs are predominantly a cargo for riboflavin, which is able to stabilize and deliver it to tumor cells for the purposes of PDT. Different alterations in the Rb-CeF_3 NPs synthesis process, variations in the ratio of components and selection of various light irradiation conditions can improve the photosensitizing capabilities of this nanomaterial.

Supplementary Materials: The following supporting information can be downloaded at the website of this paper posted on Preprints.org.

Acknowledgements: This research was funded by the Ministry of Science and Higher Education of the Russian Federation for the Institute of Theoretical and Experimental Biophysics of the Russian Academy of Sciences (State Assignment: 075-01025-23-01).

References

1. Gunaydin, G.; Gedik, M.E.; Ayan, S. Photodynamic Therapy—Current Limitations and Novel Approaches. *Front. Chem.* **2021**, *9*, doi:10.3389/fchem.2021.691697.
2. Dolmans, D.E.J.G.J.; Fukumura, D.; Jain, R.K. Photodynamic Therapy for Cancer. *Nat Rev Cancer* **2003**, *3*, 380–387, doi:10.1038/nrc1071.
3. Agostinis, P.; Berg, K.; Cengel, K.A.; Foster, T.H.; Girotti, A.W.; Gollnick, S.O.; Hahn, S.M.; Hamblin, M.R.; Juzeniene, A.; Kessel, D.; et al. Photodynamic Therapy of Cancer: An Update. *CA: A Cancer Journal for Clinicians* **2011**, *61*, 250–281, doi:10.3322/caac.20114.
4. Juarranz, Á.; Jaén, P.; Sanz-Rodríguez, F.; Cuevas, J.; González, S. Photodynamic Therapy of Cancer. Basic Principles and Applications. *Clin Transl Oncol* **2008**, *10*, 148–154, doi:10.1007/s12094-008-0172-2.
5. Brown, S.B.; Brown, E.A.; Walker, I. The Present and Future Role of Photodynamic Therapy in Cancer Treatment. *Lancet Oncol* **2004**, *5*, 497–508, doi:10.1016/S1470-2045(04)01529-3.
6. Lan, M.; Zhao, S.; Liu, W.; Lee, C.-S.; Zhang, W.; Wang, P. Photosensitizers for Photodynamic Therapy. *Advanced Healthcare Materials* **2019**, *8*, 1900132, doi:10.1002/adhm.201900132.
7. Abrahamse, H.; Hamblin, M.R. New Photosensitizers for Photodynamic Therapy. *Biochemical Journal* **2016**, *473*, 347–364, doi:10.1042/BJ20150942.
8. Konan, Y.N.; Gurny, R.; Allémann, E. State of the Art in the Delivery of Photosensitizers for Photodynamic Therapy. *Journal of Photochemistry and Photobiology B: Biology* **2002**, *66*, 89–106, doi:10.1016/S1011-1344(01)00267-6.

9. Vassie, J.A.; Whitelock, J.M.; Lord, M.S. Targeted Delivery and Redox Activity of Folic Acid-Functionalized Nanoceria in Tumor Cells. *Mol. Pharmaceutics* **2018**, *15*, 994–1004, doi:10.1021/acs.molpharmaceut.7b00920.
10. Yu, H.; Jin, F.; Liu, D.; Shu, G.; Wang, X.; Qi, J.; Sun, M.; Yang, P.; Jiang, S.; Ying, X.; et al. ROS-Responsive Nano-Drug Delivery System Combining Mitochondria-Targeting Ceria Nanoparticles with Atorvastatin for Acute Kidney Injury. *Theranostics* **2020**, *10*, 2342, doi:10.7150/thno.40395.
11. Li, H.; Liu, C.; Zeng, Y.-P.; Hao, Y.-H.; Huang, J.-W.; Yang, Z.-Y.; Li, R. Nanoceria-Mediated Drug Delivery for Targeted Photodynamic Therapy on Drug-Resistant Breast Cancer. *ACS Appl. Mater. Interfaces* **2016**, *8*, 31510–31523, doi:10.1021/acsami.6b07338.
12. Fan, Y.; Li, P.; Hu, B.; Liu, T.; Huang, Z.; Shan, C.; Cao, J.; Cheng, B.; Liu, W.; Tang, Y. A Smart Photosensitizer–Cerium Oxide Nanoprobe for Highly Selective and Efficient Photodynamic Therapy. *Inorg. Chem.* **2019**, *58*, 7295–7302, doi:10.1021/acs.inorgchem.9b00363.
13. Chukavin, N.N.; Ivanov, V.K.; Popov, A.L. Calcein-Modified CeO2 for Intracellular ROS Detection: Mechanisms of Action and Cytotoxicity Analysis In Vitro. *Cells* **2023**, *12*, 2416, doi:10.3390/cells12192416.
14. Chukavin, N.N.; Popov, A.L.; Shcherbakov, A.B.; Ivanova, O.S.; Filippova, A.D.; Ivanov, V.K. CeO2-Calcein Nanoconjugate Protective Action against H2O2-Induced Oxidative Stress in Vitro. *Nanosystems: Phys. Chem. Math.* **2022**, *13*, 308–313, doi:10.17586/2220-8054-2022-13-3-308-313.
15. Shcherbakov, A.B.; Zholobak, N.M.; Baranchikov, A.E.; Ryabova, A.V.; Ivanov, V.K. Cerium Fluoride Nanoparticles Protect Cells against Oxidative Stress. *Materials Science and Engineering: C* **2015**, *50*, 151–159, doi:10.1016/j.msec.2015.01.094.
16. Cooper, D.R.; Kudinov, K.; Tyagi, P.; Hill, C.K.; Bradforth, S.E.; Nadeau, J.L. Photoluminescence of Cerium Fluoride and Cerium-Doped Lanthanum Fluoride Nanoparticles and Investigation of Energy Transfer to Photosensitizer Molecules. *Phys. Chem. Chem. Phys.* **2014**, *16*, 12441–12453, doi:10.1039/C4CP01044B.
17. Wang, J.; Ansari, A.A.; Malik, A.; Syed, R.; Ola, M.S.; Kumar, A.; AlGhamdi, K.M.; Khan, S. Highly Water-Soluble Luminescent Silica-Coated Cerium Fluoride Nanoparticles Synthesis, Characterizations, and In Vitro Evaluation of Possible Cytotoxicity. *ACS Omega* **2020**, *5*, 19174–19180, doi:10.1021/acsomega.0c02551.
18. Chukavin, N.N.; Kolmanovich, D.D.; Filippova, A.D.; Teplonogova, M.A.; Ivanov, V.K.; Popov, A.L. Synthesis of Redox-Active Ce0.75Bi0.15Tb0.1F3 Nanoparticles and Their Biocompatibility Study in Vitro. *Nanosystems: Phys. Chem. Math.* **2024**, *15*, 260–267, doi:10.17586/2220-8054-2024-15-2-260-267.
19. Popov, A.L.; Zholobak, N.M.; Shcherbakov, A.B.; Kozlova, T.O.; Kolmanovich, D.D.; Ermakov, A.M.; Popova, N.R.; Chukavin, N.N.; Bazikyan, E.A.; Ivanov, V.K. The Strong Protective Action of Ce3+/F-Combined Treatment on Tooth Enamel and Epithelial Cells. *Nanomaterials (Basel)* **2022**, *12*, 3034, doi:10.3390/nano12173034.
20. Cheng, Y.; Xu, H.; Cao, W.; Gao, W.; Tang, B. Cerium Fluoride Nanoparticles as a Theranostic Material for Optical Imaging of Vulnerable Atherosclerosis Plaques. *Journal of the American Ceramic Society* **2023**, *106*, 2375–2383, doi:10.1111/jace.18924.
21. Chukavin, N.N.; Filippova, K.O.; Ermakov, A.M.; Karmanova, E.E.; Popova, N.R.; Anikina, V.A.; Ivanova, O.S.; Ivanov, V.K.; Popov, A.L. Redox-Active Cerium Fluoride Nanoparticles Selectively Modulate Cellular Response against X-Ray Irradiation In Vitro. *Biomedicines* **2024**, *12*, 11, doi:10.3390/biomedicines12010011.
22. Cardoso, D.R.; Libardi, S.H.; Skibsted, L.H. Riboflavin as a Photosensitizer. Effects on Human Health and Food Quality. *Food Funct.* **2012**, *3*, 487–502, doi:10.1039/C2FO10246C.
23. Rivas Aiello, M.B.; Castrogiovanni, D.; Parisi, J.; Azcárate, J.C.; García Einschlag, F.S.; Gensch, T.; Bosio, G.N.; Mártire, D.O. Photodynamic Therapy in HeLa Cells Incubated with Riboflavin and Pectin-Coated Silver Nanoparticles. *Photochemistry and Photobiology* **2018**, *94*, 1159–1166, doi:10.1111/php.12974.
24. Xu, F.; Li, J.; Zhu, T.; Yu, S.-S.; Zuo, C.; Yao, R.; Qian, H. A New Trick (Hydroxyl Radical Generation) of an Old Vitamin (B2) for near-Infrared-Triggered Photodynamic Therapy. *RSC Adv.* **2016**, *6*, 102647–102656, doi:10.1039/C6RA23440B.
25. Corbin, F. Pathogen Inactivation of Blood Components: Current Status and Introduction of an Approach Using Riboflavin as a Photosensitizer. *Int J Hematol* **2002**, *76*, 253–257, doi:10.1007/BF03165125.
26. Redmond, R.W.; Kochevar, I.E. Medical Applications of Rose Bengal- and Riboflavin-Photosensitized Protein Crosslinking. *Photochemistry and Photobiology* **2019**, *95*, 1097–1115, doi:10.1111/php.13126.

27. Khan, S.; P, M.R.; Rizvi, A.; Alam, Md.M.; Rizvi, M.; Naseem, I. ROS Mediated Antibacterial Activity of Photoilluminated Riboflavin: A Photodynamic Mechanism against Nosocomial Infections. *Toxicology Reports* **2019**, *6*, 136–142, doi:10.1016/j.toxrep.2019.01.003.
28. Yu, Y.; Yang, L.; He, C.; Tai, S.; Zhu, L.; Ma, C.; Yang, T.; Cheng, F.; Sun, X.; Cui, R.; et al. An Experimental Study on Riboflavin Photosensitization Treatment for Inactivation of Circulating HCT116 Tumor Cells. *Journal of Photochemistry and Photobiology B: Biology* **2019**, *196*, 111496, doi:10.1016/j.jphotobiol.2019.04.005.
29. Darguzyte, M.; Drude, N.; Lammers, T.; Kiessling, F. Riboflavin-Targeted Drug Delivery. *Cancers* **2020**, *12*, 295, doi:10.3390/cancers12020295.
30. Bareford, L.M.; Phelps, M.A.; Foraker, A.B.; Swaan, P.W. Intracellular Processing of Riboflavin in Human Breast Cancer Cells. *Mol. Pharmaceutics* **2008**, *5*, 839–848, doi:10.1021/mp800046m.
31. Suwannasom, N.; Kao, I.; Pruß, A.; Georgieva, R.; Bäumler, H. Riboflavin: The Health Benefits of a Forgotten Natural Vitamin. *International Journal of Molecular Sciences* **2020**, *21*, 950, doi:10.3390/ijms21030950.
32. Pinto, J.T.; Zempleni, J. Riboflavin. *Adv Nutr* **2016**, *7*, 973–975, doi:10.3945/an.116.012716.
33. Remucal, C.K.; McNeill, K. Photosensitized Amino Acid Degradation in the Presence of Riboflavin and Its Derivatives. *Environ. Sci. Technol.* **2011**, *45*, 5230–5237, doi:10.1021/es200411a.
34. Insińska-Rak, M.; Sikorski, M.; Wolnicka-Glubisz, A. Riboflavin and Its Derivates as Potential Photosensitizers in the Photodynamic Treatment of Skin Cancers. *Cells* **2023**, *12*, 2304, doi:10.3390/cells12182304.
35. Lee, T.Y.; Farah, N.; Chin, V.K.; Lim, C.W.; Chong, P.P.; Basir, R.; Lim, W.F.; Loo, Y.S. Medicinal Benefits, Biological, and Nanoencapsulation Functions of Riboflavin with Its Toxicity Profile: A Narrative Review. *Nutrition Research* **2023**, *119*, 1–20, doi:10.1016/j.nutres.2023.08.010.
36. Beztsinna, N.; Solé, M.; Taib, N.; Bestel, I. Bioengineered Riboflavin in Nanotechnology. *Biomaterials* **2016**, *80*, 121–133, doi:10.1016/j.biomaterials.2015.11.050.
37. Rivas Aiello, M.B.; Romero, J.J.; Bertolotti, S.G.; Gonzalez, M.C.; Mártire, D.O. Effect of Silver Nanoparticles on the Photophysics of Riboflavin: Consequences on the ROS Generation. *J. Phys. Chem. C* **2016**, *120*, 21967–21975, doi:10.1021/acs.jpcc.6b06385.
38. Akasov, R.A.; Sholina, N.V.; Khochenkov, D.A.; Alova, A.V.; Gorelkin, P.V.; Erofeev, A.S.; Generalova, A.N.; Khaydukov, E.V. Photodynamic Therapy of Melanoma by Blue-Light Photoactivation of Flavin Mononucleotide. *Sci Rep* **2019**, *9*, 9679, doi:10.1038/s41598-019-46115-w.
39. Machado, D.; Shishido, S.M.; Queiroz, K.C.S.; Oliveira, D.N.; Faria, A.L.C.; Catharino, R.R.; Spek, C.A.; Ferreira, C.V. Irradiated Riboflavin Diminishes the Aggressiveness of Melanoma In Vitro and In Vivo. *PLOS ONE* **2013**, *8*, e54269, doi:10.1371/journal.pone.0054269.
40. Ohara, M.; Fujikura, T.; Fujiwara, H. Augmentation of the Inhibitory Effect of Blue Light on the Growth of B16 Melanoma Cells by Riboflavin. *International Journal of Oncology* **2003**, *22*, 1291–1295, doi:10.3892/ijo.22.6.1291.
41. Chen, Z.; Huang, S.; Liu, M. The Review of the Light Parameters and Mechanisms of Photobiomodulation on Melanoma Cells. *Photodermatology, Photoimmunology & Photomedicine* **2022**, *38*, 3–11, doi:10.1111/phpp.12715.